Inorg. Chem. **2006**, *45*, 8664–8671

Cadmium(II) and Zinc(II) Complexes of *S*-Confused Thiaporphyrin

Michał J. Chmielewski, Miłosz Pawlicki, Natasza Sprutta, Ludmiła Szterenberg, and Lechosław Latos-Grażyński*

Department of Chemistry, University of Wroclaw, 14 F. Joliot-Curie Street, Wrocław 50 383, Poland

Received June 17, 2006

The synthesis of 5,10,15,20-tetraphenyl-2-thia-21-carbaporphyrin [*S*-confused thiaporphyrin, (*SCPH*)H] was optimized. The formation of the phlorin was detected, which was saturated at the meso carbon adjacent to thiophene. Phlorin converted readily to (*SCPH*)H in the final oxidation process. Insertion of cadmium(II) and zinc(II) into *S*-confused thiaporphyrin yielded (*SCPH*)Cd^{II}Cl and (*SCPH*)Zn^{II}Cl complexes. The macrocycle acted as a monoanionic ligand. Three nitrogen atoms and the C(21)H fragment of the inverted thiophene occupied equatorial positions. The compensation of the metal charge required the apical chloride coordination. The characteristic C(21)H resonances of the inverted thiophene ring were located at 1.71 and 1.86 ppm in the ^{1}H NMR spectra of (*SCPH*)Cd^{II}Cl and (*SCPH*)Zn^{II}Cl, respectively. The proximity of the thiophene fragment to the metal ion induced direct scalar couplings between the spin-active nucleus of the metal ($^{111/113}$Cd) and the adjacent ^{1}H nucleus (J_{CdH} = 8.97 Hz). The interaction of the metal ion and C(21)H also was reflected by significant changes of C(21) chemical shifts: (*SCPH*)Zn^{II}Cl, 92.9 ppm and (*SCPH*)Cd^{II}Cl, 88.2 ppm (free ligand (*SCPH*)H, 123.7 ppm). The X-ray analysis performed for (*SCPH*)-Cd^{II}Cl confirmed the side-on cadmium–thiophene interaction. The Cd···C(21) distance (2.615(7) Å) exceeded the typical Cd–C bond lengths, but was much shorter than the corresponding van der Waals contact. The density functional theory (DFT) was applied to model the molecular structures of zinc(II) and cadmium(II) complexes of *S*-confused thiaporphyrin. Subsequent AIM analysis demonstrated that the accumulation of electron density between the metal and thiophene, which is necessary to induce these couplings, was fairly small. A bond path linked the cadmium(II) ion to the proximate C(22) carbon of the thiophene.

Introduction

A heteroatom confusion (*X*-confusion) concept, which was originally exemplified by a porphyrin−2-aza-21-carbaporphyrin couple **1**,[1,2] can be applied in construction of a nontrivial macrocyclic environment for organometallic chemistry. Thus, interchanging a heteroatom with a β-methine group transforms the regular 21-*X*-heteroporphyrin into its "*X*-confused" isomer.[3,4] Alternatively, by analogy to a regular heteroporphyrin formal construction, one can replace the outer nitrogen of *N*-confused porphyrin **1** with a heteroatom of choice. This strategy resulted in the formation of thia-**3**,[5,6] and oxa-analogues **2**[7,8] of *N*-confused porphyrin **1** in which the sulfur or oxygen is placed at a macrocyclic perimeter. The carbon atom of the heterocyclic subunit is directed toward a center of a macrocyclic crevice (Chart 1).

Previously following such an approach, we have characterized *O*-confused oxaporphyrin **2**, albeit in its dicationic form,[7] and *S*-confused thiaporphyrin **3**.[5] In contrast to *S*-confused thiaporphyrin **3**, the oxa-analogue **2** is extremely reactive toward nucleophilic attack at peripheral position 3, which results in aromatization of the macrocycle, and the formation of derivatives such as **4** and **5**, which are both formally related to the product of 2-oxa-21-carbaporphyrin hydrogenation.[7,8] Thus, macrocyclic delocalization and aromaticity in **2** is easily switched on and off by the reversible addition/elimination of a nucleophile at the position C(3), coupled with tetrahedral−trigonal conversion of the C(3) carbon.

* To whom correspondence should be addressed. E-mail: llg@wchuwr.chem.uni.wroc.pl.

(1) Chmielewski, P. J.; Latos-Grażyński, L.; Rachlewicz, K.; Głowiak, T. *Angew. Chem., Int. Ed. Engl.* **1994**, *33*, 779.
(2) Furuta, H.; Asano, T.; Ogawa, T. *J. Am. Chem. Soc.* **1994**, *116*, 767.
(3) Pawlicki, M.; Latos-Grażyński, L. *Chem. Rec.* **2006**, *6*, 64.
(4) Furuta, H.; Maeda, H.; Osuka, A. *Chem. Commun.* **2002**, 1795.
(5) Sprutta, N.; Latos-Grażyński, L. *Tetrahedron Lett.* **1999**, *40*, 8457.
(6) Szterenberg, L.; Sprutta, N.; Latos-Grażyński, L. *J. Inclusion Phenom.* **2001**, *41*, 209.
(7) Pawlicki, M.; Latos-Grażyński, L. *J. Org. Chem.* **2005**, *70*, 9123.
(8) Pawlicki, M.; Latos-Grażyński, L. *Chem.—Eur. J.* **2003**, *9*, 4650.

10.1021/ic061091p CCC: $33.50
Published on Web 09/15/2006

Chart 1. *X*-Confused Heteroporphyrins

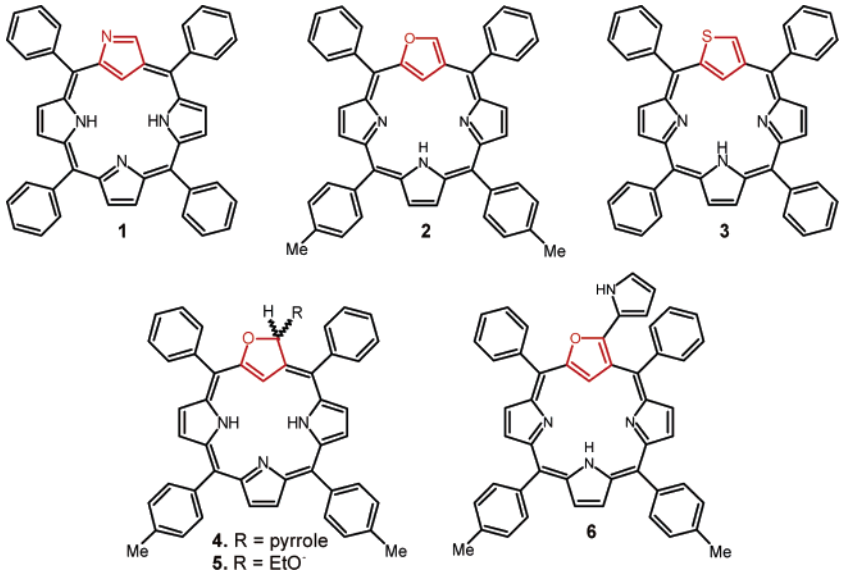

The construction of carbaporphyrinoids obtained in the course of *X*-confusion opens a way for a potential accommodation of a large variety of metal ions that allows an exploration of organometallic complexes in a porphyrin-like environment.[3] In particular, the coordination properties of the first reported carbaporphyrinoid, *N*-confused carbaporphyrin **1**, was explored for a large variety of metal ions.[4,9−11] Flexibility of the inverted porphyrin results in formation of various coordination modes in macrocyclic environments with or without the formation of a direct metal−carbon bond.[1,12,13] Importantly, atypical oxidation states of metal ions trapped in organometallic environments have been detected.[11,14−17] Coordination chemistry of *O*-confused carbaporphyrins reported for the limited number of metal ions resembles that of *N*-confused porphyrin. Thus, insertion of metal ions into *O*-confused carbaporphyrin derivatives afforded organometallic complexes of **6** [Ag(III), Ni(II), Pd(II)],[8] **2** [Ag(III)],[7] and **5** [Ag(III)].[7] Coordination of nickel(II) or palladium(II) by **4** is accompanied by the dehydrogenation step which results in the formation of a "true" *O*-confused oxaporphyrin frame of **6** but with an appended pyrrole. Essentially, the oxidation of the central metal ion was considered as a factor that determines the molecular structure of the ligand. Thus, the dianionic or trianionic macrocyclic core of pyrrole appended derivatives have been adjusted to match the oxidation state of nickel(II), palladium(II), and silver(III), respectively.[8] The pyrrole appended *O*-confused carbaporphyrin **6** acts as a monoanionic ligand toward zinc(II) and cadmium(II) cations. Three nitrogen atoms and the C(21)H fragment of the inverted furan occupy equatorial positions. The proximity of the furan fragment to the metal ion induces direct scalar couplings between the spin-active nucleus of the metal ($^{111/113}$Cd) and the adjacent ^{1}H nucleus.[18] The coordination properties also were explored for other carbocyclic analogues: *m*-benziporphyrin,[19−22] azuliporphyrin,[23] and benzocarbaporphyrin.[24]

Here, we present the formation and characterization of cadmium(II) and zinc(II) complexes of *S*-confused carbaporphyrin **3**, which acts as a monoanionic ligand. Consequently, a side-on coordination mode of *S*-confused carbaporphyrin was detected, which affords an interaction between the metal ion and the C(21)H unit of inverted thiophene. The goal of the present work was to investigate metal−thiophene interactions in complexes and to show how this weak bonding affects NMR spectroscopic parameters. This experimental approach exploits our previous finding[18,19,21,25] that the proximity of the metal ion and arene gives rise to observable ^{1}H−X and ^{13}C−X scalar couplings in the NMR spectra. Such couplings are usually classified as through-space or nonbonding, because their magnitude cannot be rationalized in terms of the network of formal bonds in the

(9) Latos-Grażyński, L. Core Modified Heteroanalogues of Porphyrins and Metalloporphyrins. In *The Porphyrin Handbook*; Kadish, K. M., Smith, K. M., Guilard, R., Eds.; Academic Press: New York, 2000; pp 361−416.
(10) Harvey, J. D.; Ziegler, C. J. *Chem. Commun.* **2002**, 1942.
(11) Chmielewski, P. J.; Latos-Grażyński, L. *Coord. Chem. Rev.* **2005**, *249*, 2510.
(12) Chmielewski, P. J.; Latos-Grażyński, L.; Głowiak, T. *J. Am. Chem. Soc.* **1996**, *118*, 5690.
(13) Furuta, H.; Morimoto, T.; Osuka, A. *Inorg. Chem.* **2004**, *43*, 1618.
(14) Chmielewski, P. J.; Latos-Grażyński, L. *Inorg. Chem.* **1997**, *36*, 840.
(15) Chmielewski, P. J.; Latos-Grażyński, L.; Schmidt, I. *Inorg. Chem.* **2000**, *39*, 5475.
(16) Furuta, H.; Ogawa, T.; Uwatoko, Y.; Araki, K. *Inorg. Chem.* **1999**, *38*, 2676.
(17) Maeda, H.; Ishikawa, Y.; Matsuda, T.; Osuka, A.; Furuta, H. *J. Am. Chem. Soc.* **2003**, *125*, 11822.
(18) Pawlicki, M.; Latos-Grażyński, L.; Szterenberg, L. *Inorg. Chem.* **2005**, *44*, 9779.
(19) Stępień, M.; Latos-Grażyński, L. *Acc. Chem. Res.* **2005**, *38*, 88.
(20) Hung, C.-H.; Chang, F.-C.; Lin, C.-Y.; Rachlewicz, K.; Stępień, M.; Latos-Grażyński, L.; Lee, G.-H.; Peng, S.-M. *Inorg. Chem.* **2004**, *43*, 4118.
(21) Stępień, M.; Latos-Grażyński, L.; Szterenberg, L.; Panek, J.; Latajka, Z. *J. Am. Chem. Soc.* **2004**, *126*, 4566.
(22) Stępień, M.; Latos-Grażyński, L. *Chem.—Eur. J.* **2001**, *7*, 5113.
(23) Lash, T. D.; Colby, D. A.; Graham, S. R.; Ferrence, G. M.; Szczepura, L. F. *Inorg. Chem.* **2003**, *42*, 7326.
(24) Lash, T. D.; Rasmussen, J. M.; Bergman, K. M.; Colby, D. A. *Org. Lett.* **2004**, *6*, 549.
(25) Stępień, M.; Latos-Grażyński, L. *J. Am. Chem. Soc.* **2002**, *124*, 3838.

Scheme 1. Formation of *S*-Confused Thiaporphyrin

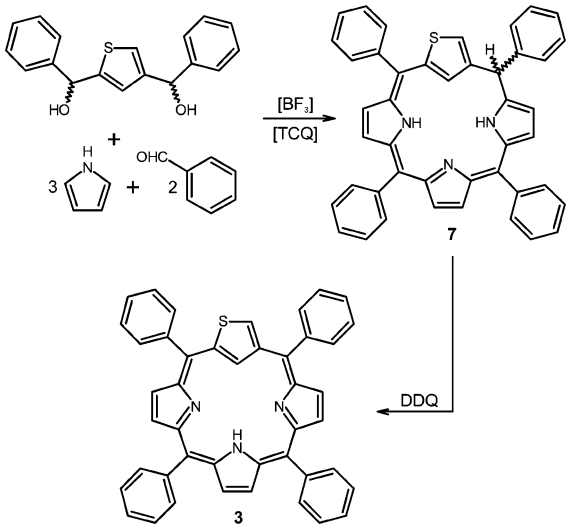

molecule.[26] Here, couplings with the spin-active nuclei of ^{111}Cd and ^{113}Cd ($I = 1/2$) are used to detect the unusual metal−thiophene interaction.[27]

Results and Discussion

Synthesis of 2-Thia-21-carbaporphyrin. As described previously, the condensation of 2,4-bis(phenylhydroxymethyl)thiophene with pyrrole and benzaldehyde (1:3:2 molar ratio) via a one pot, two-step, room temperature synthesis yielded 5,10,15,20-tetraphenyl-2-thia-21-carbaporphyrin (*SCPH*)H.[5]

In the present studies, the condensation processes were optimized, which allowed the improved yield of 10% (see experimental section). The detailed analysis of the condensation products also resulted in identification of phlorin **7**, which readily converted into the target macrocycle **3** during the oxidation process (Scheme 1). Phlorin **7** showed spectroscopic properties that were typical for phlorin-like molecules.[22,28,29] Several two-dimensional (2D) experiments (COSY, NOESY, HMQC, HMBC) were involved to solve the structure of **7**. The assignment of signal shown in Figure 1 was performed based on a combination of COSY and NOESY experiments, which took a unique NOE contact between H(3) and meso-H(5) as a starting point. Tetrahedral geometry around the C(5) atom completely blocked the π-delocalization. Thus, **7** demonstrated nonaromatic character that had predictable consequences in spectroscopic parameters. The ^{1}H NMR spectrum of **7** contained three AB systems assigned to the β-pyrrolic protons: H(18) 6.88, H(17) 6.74 ppm ($^3J = 4.9$ Hz); H(12) 6.83, H(13) 6.49 ppm ($^3J = 4.9$ Hz); and H(7) 6.62, H(8) 6.59 ppm ($^3J = 4.9$ Hz). The thiophene resonances were observed at 7.56 ppm [H(3)] and 5.93 ppm [H(21)]. The structurally informative H(5) resonance for **7** was identified at 5.99 ppm. This hydrogen

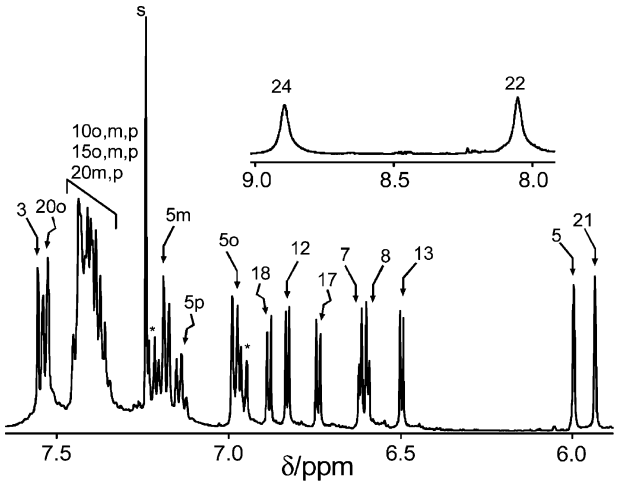

Figure 1. ^{1}H NMR spectrum of **7** ($CDCl_3$, 298 K). The inset presents downfield region with NH protons. Peak labels follow systematic position numbering of the macrocycle or denote proton groups: o, m, p (ortho, meta, and para positions of *meso*-phenyl (Ph), respectively).

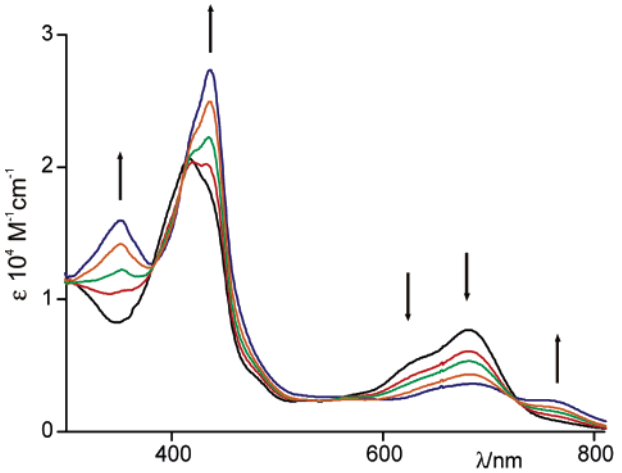

Figure 2. Oxidation of **7** with DDQ as followed by UV−vis spectroscopy. **7**, black line; **3**, blue line.

was bound to the tetrahedral C(5) carbon atom as the ^{13}C chemical shift of C(5) (46.8 ppm) was consistent with the tetrahedral hybridization. The direct correlation between H(5) and C(5) resonances was detected in the HMQC map. Two NH resonances at 8.05 ppm [N(22)H] and 8.90 ppm [N(24)H] were identified in the ^{1}H NMR spectrum of **7**. The COSY experiment in which scalar couplings already were assigned between the β-protons and appropriate NH resonances allowed the unambiguous localization of the NH hydrogens. Accordingly, a single tautomer (Scheme 1) was identified in solution.

The UV−vis spectra presented the pattern typical for nonaromatic porphyrin derivatives. In particular, the extinction coefficients ($\epsilon \approx 8 \times 10^3$) confirmed the absence of the aromaticity. The electronic spectra resembled those of *m*-benziporphyrin[22] or 3-aza-*m*-benziporphyrin (*N*-confused pyriporphyrin).[29] Titration of **7** with 2,3-dichloro-5,6-dicyanobenzoquinone (DDQ) monitored with UV−vis shows the smooth transformation of phlorin into *S*-confused thiaporphyrin **3** (Figure 2).

Coordination Compounds of *S*-Confused Carbaporhyrin. Insertion of cadmium(II) and zinc(II) was achieved by

(26) Hilton, J.; Sutcliffe, L. H. *Prog. Nucl. Magn. Reson. Spectrosc.* **1975**, *10*, 27.
(27) Contreras, R. H.; Facelli, J. C. *Annu. Rep. NMR Spectrosc.* **1993**, *27*, 255.
(28) Krattinger, B.; Callot, H. J. *Chem. Commun.* **1996**, 1341.
(29) Myśliborski, R.; Latos-Grażyński, L. *Eur. J. Org. Chem.* **2005**, 5039.

Scheme 2. Insertion of Metal Ions

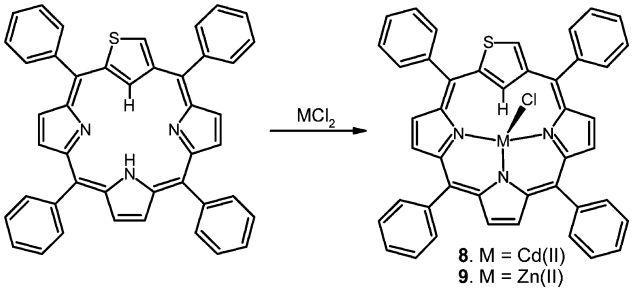

boiling the free base **3** and an appropriate metal chloride (anhydrous) in either chloroform [cadmium(II)] or tetrahydrofuran (THF) [zinc(II)] (Scheme 2). The resulting complexes were obtained in quantitative yield.

The UV−vis spectra of **8** and **9** are shown in Figure 3. In both cases, very similar patterns were observed. This suggested a similar structure for the cadmium **8** and zinc **9** complexes.

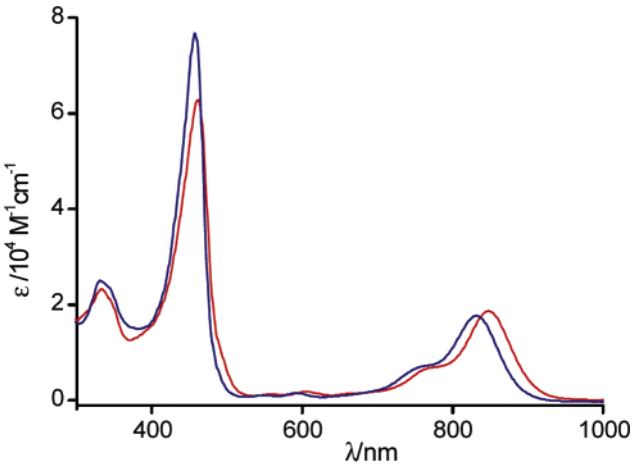

Figure 3. The UV−vis spectra of **8** (red) and **9** (blue) in CH_2Cl_2.

The cadmium and zinc complexes presented a side-on coordination mode in which the metal ion was bound by three nitrogen atoms with an interaction between the central ion and sustained C(H) unit of the inverted thiophene (Scheme 2). Thus, the macrocycle acted as a monoanionic ligand, and the metal ion required coordination of the axial chloride for compensation of the metal charge. The ^{1}H NMR spectra confirmed the side-on coordination mode (Figure 4). Significantly, the β-pyrrolic signals were relocated slightly downfield (8.1−7.5 ppm) in comparison to the signals of the free ligand (7.2−6.8 ppm). Contrary to perimeter resonances, the marked upfield relocation had been detected for the inner H(21) unit (**8**, **9**, and **3** at 1.71, 1.86, and 4.8 ppm, respectively). The adjacency of the C(21)H unit and the cadmium(II) ion induced the scalar couplings between the proton and the NMR active isotopes of cadmium ($^{111/113}$Cd), which were observed directly in the ^{1}H NMR spectra (Figure 4B). This interaction between the metal ion and proton resulted in the C(21)H characteristic pattern (Figure 4A, inset). Significantly, the $^{111/113}$Cd−^{1}H interaction ($J_{CdH} \approx 9.0$ Hz) was too effective to explain this just based on the normal through bond coupling, especially when both

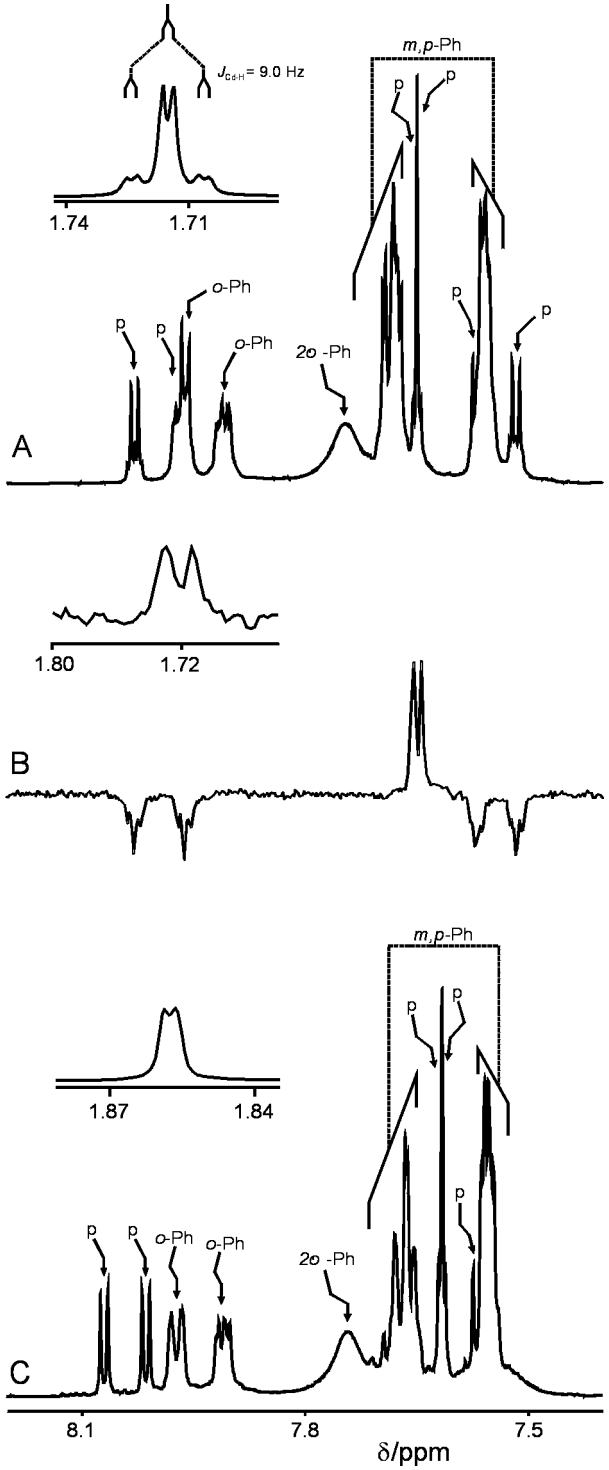

Figure 4. ^{1}H NMR spectra of **8** (A) and **9** (C) ($CDCl_3$, 298K). (B) 1D gsHSQC for **8**. Insets demonstrate the zoomed H(21) region. Peak labels: p = pyrrole; *o*-Ph, *m*-Ph, *p*-Ph are ortho, meta and para positions respectively, of *meso*-phenyl (Ph).

interacting parts were six bonds apart and the geometry was unfavorable. The presence of this type of interaction reflected the spatial proximity between the cadmium and the C(21)H unit of *S*-confused thiophene. The coupling constant was slightly smaller than the J_{CdH} value observed for cadmium(II) *O*-confused carbaporphyrin with a pendant pyrrole ring (10.7 Hz)[18] but was larger in comparison to cadmium(II) *m*-benziporphyrin (7.4 Hz).[21] The detailed analysis of the

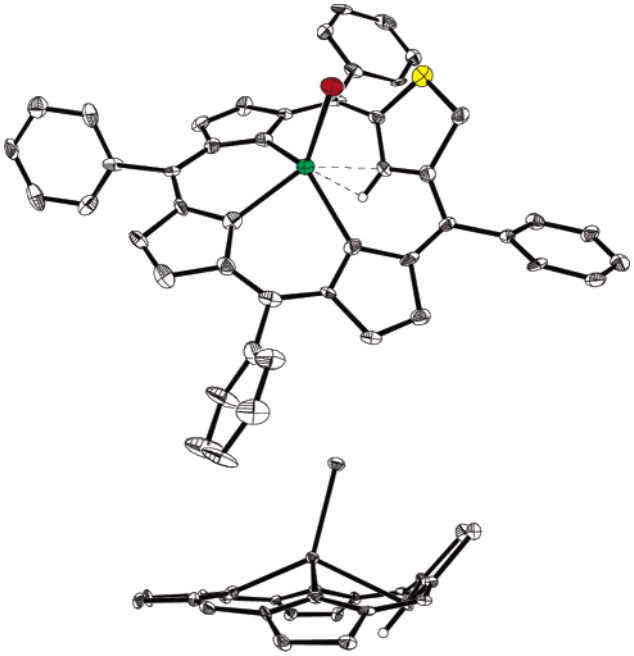

Figure 5. Crystal structure of **8**. The upper trace presents the perspective view, and the bottom trace represents the side view (aryl substituents are omitted for clarity).

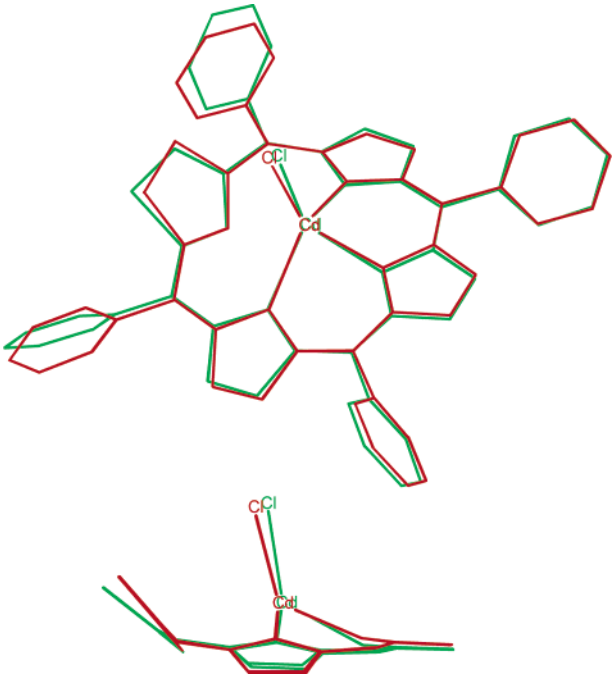

Figure 6. Comparison of X-ray and DFT geometries (red and green, respectively) for **8**.

^{1}H and ^{13}C NMR spectra also allowed the estimation of the normal through bond scalar coupling values in the pyrrole frame: $^2J_{Cd-C} = 4-6$ Hz, $^3J_{Cd-C} = 10-12$ Hz, and $^4J_{Cd-H} = 4-5$ Hz. The interaction of the metal ion and C(21)H unit also was reflected in the carbon chemical shifts. The C(21) resonances for **8** and **9** were observed at 88.7 and 92.9 ppm, respectively. Thus, they experienced remarkable upfield relocation in comparison to the starting macrocycle (123.7 ppm). The analogical influence of interaction on the ^{13}C chemical shift was previously detected for cadmium(II) and zinc(II) complexes of the *O*-confused carbaporphyrin,[18] the dimeric complexes of *N*-confused carbaporphyrin,[13] and the monomeric zinc(II) complex of *N*-confused porphyrin.[30] Actually, the upfield relocation of the inner carbon resonance involved in interaction (increments up to 27 ppm) also was observed for the carbon atom of cadmium(II), zinc(II), and mercury(II) *m*-benziporphyrin complexes.[21] For the sake of comparison, we would like to note that the coordinated internal carbon atom acquires tetrahedral geometry, which was observed for nickel(II) complexes of alkylated[31] and protonated *N*-confused carbaporphyrin[32] yields the resonance at around 33 ppm.

Crystal Structure of 8. X-ray analysis has been performed for **8**. The perspective views of **8** are presented in Figure 5. The crystallographic view was consistent with spectral observations. A central ion was bounded by three pyrrolic donors with an apical chloride.

The *S*-confused cadmium(II) complex, **8**, crystallized in space group $P\bar{1}$. The coordinating environment of Cd(II) formed a trigonal bipyramid with the N(23) atom, chloride, and C(21)−H bond occupying the equatorial positions. The Cd−N [Cd−N(22), 2.296(6) Å, Cd−N(23), 2.191(6) Å, Cd−N(24), 2.279(6) Å] and Cd−Cl (Cd−Cl, 2.413(2) Å) bond lengths were directly comparable to those reported for *m*-,[21] and *p*-benziporphyrin[25] cadmium complexes, although the trans Cd−N bond was systematically shorter than the other two Cd−N distances. The cadmium(II) ion was displaced from the N_3 plane by ca. 0.87 Å toward the chloride, which was comparable to the *m*-benziporphyrin complex,[21] but it was significantly larger than in the cadmium(II) *p*-benziporphyrin complex.[25] The *S*-confused thiophene approached the cadmium(II) ion. The Cd···C(21) and Cd···H(21) distances equaled 2.615(7) and 2.56 Å, respectively. The Cd···C(21) distance in **8** was much smaller than the corresponding van der Waals contact (3.3 Å),[33] but it exceeded the typical Cd−C bond lengths (2.10−2.35 Å).[34] The dihedral angle between the N_3 and thiophene planes was equal to 49.4°.

Atoms in Molecules (AIM) Analysis of Cadmium(II) *S*-Confused Thiaporphyrin. The observation of scalar coupling between the Cd nucleus and thiophene protons in **8** indicated that there must be a certain accumulation of electron density between the metal and the arene to transmit the coupling. However, NMR data did not explain the nature of the metal−thiophene interaction.

Calculations were performed for the cadmium(II) complex of **3**. It was necessary to include *meso*-aryl substituents in the calculations although it required a substantial computational effort. Previously, we found that the absence of *meso*-aryls produces the substantial differences in the optimized

(30) Furuta, H.; Ishizuka, T.; Osuka, A. *J. Am. Chem. Soc.* **2002**, *124*, 5622.
(31) Schmidt, I.; Chmielewski, P. J. *Chem. Commun.* **2002**, 92.
(32) Schmidt, I.; Chmielewski, P. J.; Ciunik, Z. *J. Org. Chem.* **2002**, *67*, 8917.
(33) Bondi, A. *J. Phys. Chem.* **1964**, *68*, 441.
(34) Hursthouse, M. B.; Motevalli, M.; O'Brien, P.; Walsh, J. R.; Jones, A. C. *Organometallics* **1991**, *10*, 3196.

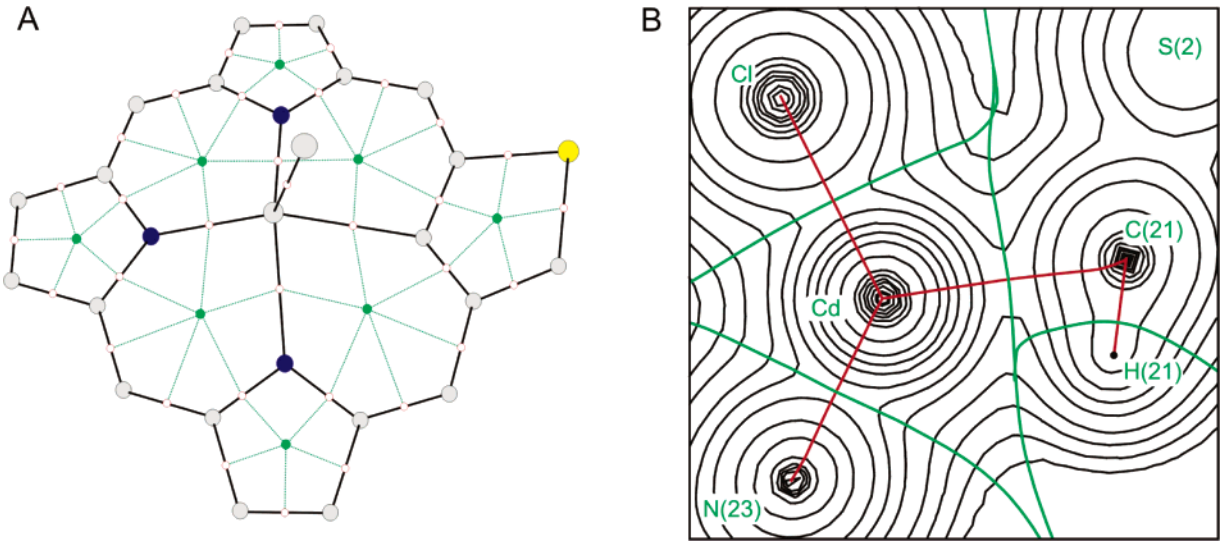

Figure 7. Connectivity of critical points in the theoretical electron densities of **8**. Bond critical points are shown in red. Black lines are approximations of bond paths. Ring critical points and their connectivity (dashed lines) are shown in green. Panel B shows the electron density distributions in **8** [in the plane of atoms Cd, Cl, and C(21)]. Green and red lines denote boundaries of atomic basins and bond paths, respectively.

macrocyclic geometry.[21,35,36] The DFT-optimized structure (B3LYP/LANL2DZ) of **8** was very similar to the X-ray geometry (Figure 6) except for the orientation of the *S*-confused thiophene ring. This ring was closer to coplanarity with the N_3 plane in the DFT model rather than in the crystal structure with the SC_4/N_3 interplanar angles being 49.4 and 36.2°, respectively. This difference probably was caused by intermolecular interactions in the solid state rather than by deficiencies of the calculation method, and it reflected the inherent flexibility of the *S*-confused thiaporphyrin. As a result of the different tilt, the Cd···C(21) and Cd···H(21) distances in the DFT structure became 2.74 and 2.62 Å, respectively, (the values in the X-ray structure were 2.615(7) and 2.56 Å, respectively). The DFT-optimized structure also was obtained for **9**. The resultant geometry was almost identical to **8** (see Supporting Information). Apparently, the DFT structure overemphasized the agostic character of the Cd−arene interaction. However, we have decided to use this DFT model of **8** for the AIM analysis because (vide infra) the X-ray geometry does not correspond to a numerical energy minimum, which is required by the theory of AIM.[37]

The theory of AIM developed by Bader[37] derives chemically relevant information from the topology of electron density in a molecule. In particular, it describes chemical bonding in terms of bond critical points (BCPs) and bond paths and provides an unambiguous scheme of partitioning molecules into atoms (atomic basins). Figure 7 shows the connectivity of critical points in structures of **8**, as well as important cross sections of the electron density. Numerical properties of selected critical points are given in Table 1 (see Supporting Information for additional data). The topology of electron density in **8** agrees with chemical expectations (Figure 7A); each BCP is associated with a bond, and that there are eight ring points (thiophene ring, three pyrrole rings, and the four inner rings formed upon the binding of cadmium). Most important of all, there is a bond critical point between the cadmium(II) ion and thiophene. The bond path passing through this point connects cadmium and C(21) (Figure 7B).

Table 1. Parameters of Selected Bond Critical Points (BCPs) Obtained from the AIM Analyses of **8** (au or dimensionless)[a]

	ρ	∇^2_ρ	H	B
Cd − Cl	0.0526	0.1807	−0.0073	0.2553
Cd···C(21)	0.0228	0.0633	−0.0026	0.0107
Cd − N(24)	0.0551	0.2453	−0.0056	0.0643
Cd − N(23)	0.0628	0.2997	−0.0067	0.0663
Cd − N(22)	0.0540	0.2378	−0.0055	0.0623
C(4) − C(5)	0.2907	−0.7735	−0.2903	1.5411
Cd···C(22)[21]	0.0186	0.0637	−0.0002	0.0100

[a] Explanation of symbols: ρ, electron density at BCP; ∇^2_ρ, Laplacian; H, total energy density; B, Wiberg bond index.

Comparison of the properties of various bond critical points is helpful in discussing the metal−thiophene interaction in cadmium(II) *S*-confused thiaporphyrin. The data gathered in Table 1 provide examples of a typical covalent bond (C−C), bonds with a high degree of ionicity [Cd−N, Cd−Cl, and the metal−thiophene interaction itself (Cd··· C(21)]. Evidently, the metal-thiophene interaction only has a weak bonding character. The density ρ at the respective BCP in **8** equals 0.025 au. Correspondingly, bond orders B calculated for the Cd···C contacts according to the Wiberg method[38] are significantly lower than the Cd−N and Cd−Cl bond orders.

A unique feature of AIM is that it is able to quantify the degree of electron sharing. The most commonly used measure is the Laplacian of electron density ∇^2_ρ in conjunction with the ρ value at a BCP.[39] Covalent bonds (shared interactions) are characterized by ρ values exceeding 0.1 au, while ∇^2_ρ can be negative (nonpolar bonds) or positive (certain polar bonds, such as C═O). For ionic bonds, H-bonds, and in van der Waals molecules (closed-shell interactions), the density ρ is in the range from 10^{-3} to 10^{-2}

(35) Szterenberg, L.; Latos-Grażyński, L. *THEOCHEM* **1999**, *490*, 33.
(36) Stępień, M.; Latos-Grażyński, L.; Szterenberg, L. *Inorg. Chem.* **2004**, *43*, 6654−6662.
(37) Bader, R. F. W. *Atoms in Molecules − a Quantum Theory*; Oxford University Press: Oxford, 1990.

au, while the Laplacian is always positive. In this sense, agostic bonds are of the closed-shell type ($\rho = 0.04-0.05$ au, $\nabla^2\rho = 0.15-0.25$ au).[40]

The values given in Table 1 agree with the previously reported data. The Cd−N and Cd−Cl bonds are largely ionic, which is in contrast to the covalent bonds of the macrocycle, as exemplified by C(4)−C(5). The Cd···C(21) interaction is characterized by ρ and ∇^2_ρ values, which are comparable with the results obtained for hydrogen bonds.[41] A complementary parameter proposed to classify bonding types is the total electronic energy density H at the BCP.[42] Negative H values have been associated with electron sharing, and positive values with closed-shell interactions. All H values given in Table 1 are negative. However, the absolute values of H obtained for Cd···C(21) interactions and ionic bonds are very small, so that the degree of electron sharing must be considered insignificant. The Cd···C(21) interaction characterized in terms of AIM resembles one previously described for cadmium(II) *m*-benziporphyrin (Table 1) despite the obvious differences between involved aromatic rings.[21]

Conclusion

An *S*-confusion concept was applied to construct a nontrivial macrocyclic platform for organometallic chemistry. The combination of structural motifs in *S*-confused thiaporphyrin provides a unique opportunity to study weak metal−thiophene interactions. The metal ion, which is bound by the tripyrrolic brace, is brought into the vicinity of the thiophene, and the resulting complex has been investigated by spectroscopic methods or X-ray crystallography. In the present paper, we have described spectroscopic manifestations of the metal−thiophene interactions observed in the diamagnetic zinc(II) and cadmium(II) *S*-confused thiaporphyrin complexes. The interaction led to scalar coupling between the spin-active metal nucleus (^{111}Cd, ^{113}Cd) and the proximate ^{1}H and ^{13}C nuclei of the thiophene. The couplings were transmitted despite the absence of a formal Cd−thiophene bond.

DFT calculations performed for cadmium(II) species and subsequent AIM analysis show that the accumulation of electron density between the metal and arene that is necessary to induce the scalar couplings is fairly small. Significantly, a bond path links the cadmium(II) ion to the proximate carbon of the thiophene.

Systematic investigation of appropriately modified systems may help in quantifying the relationship between bonding strength and the spectroscopic probes described in this paper. At present, we conclude that cadmium(II) complexes of *O*-confused and *S*-confused heteroporphyrins reveal similar interactions despite the obvious differences in the nature of *X*-confused fragments.

(38) Wiberg, K. B. *Tetrahedron* **1968**, *24*, 1083.
(39) Bader, R. F. W. *J. Phys. Chem.* **1996**, *100*, 10892.
(40) Popelier, P. L. A.; Logothetis, G. *J. Organomet. Chem.* **1998**, *555*, 101.
(41) Popelier, P. L. A. *Atoms in Molecules. An Introduction*; Pearson Education: Harlow, U.K., 2000.
(42) Cremer, D.; Kraka, E. *Angew. Chem., Int. Ed. Engl.* **1984**, *23*, 627.

Experimental Section

Solvents and Reagents. Dichloromethane-d_2 (CIL) was used as received. Chloroform-*d* (CIL) passed through basic Al_2O_3. Thiophene, *n*-BuLi, *s*-BuLi, and $BF_3{\cdot}Et_2O$ were used as received. 2,4-Bis-(phenylhydroxymethyl)thiophene was obtained as previously described.[5]

5,10,15,20-Tetraphenyl-2-thia-21-carbaporphyrin 3. The solution of 2,4-bis-(phenylhydroxymethyl)thiophene (296 mg, 1.00 mmol) in 150 mL of CH_2Cl_2 (freshly distilled from CaH_2) was deoxygenated with a gentle stream of nitrogen for 15 min. Subsequently, pyrrole (201 mg, 3.00 mmol) and benzaldehyde (212 mg, 2.00 mmol) were added. The resulting mixture was deoxygenated for an additional 20 min. After this time, $BF_3{\cdot}Et_2O$ (195 μL) was added, and the reaction mixture was stirred with protection from light. After 1 h, *p*-chloranil (987 mg) was added, and the resulting mixture was refluxed for another 1 h. The solvent was removed by rotary evaporator, and the resulting dark residue was dissolved in a small volume of freshly distilled CH_2Cl_2 (most of tars remain undissolved). The solution was chromatographed on 200 g of deactivated Al_2O_3 (GII) using CH_2Cl_2 as an eluent followed by 0.5% CH_3OH in CH_2Cl_2 until tars appeared. Fractions containing green solution of the desired product were collected, evaporated, and immediately chromatographed again on 200 g of active Al_2O_3 using gradient elution with toluene/CH_2Cl_2 mixtures. Tetraphenylporphyrin (TPP) was eluted as the first product using a toluene/CH_2Cl_2 (1:1) mixture and finally with CH_2Cl_2. Then the desired product was washed out with 0.5% MeOH in CH_2Cl_2. All fractions containing **3** were collected and evaporated. The product was finally purified by precipitation from concentrated CH_2Cl_2 solution with methanol. Yield 63 mg (10%). The product has identical spectroscopic properties to those previously described.[5]

5,10,15,20-Tetraphenyl-5-hydro-2-thia-21-carbaphlorin 7. The following modifications in the above procedure allowed for isolation of phlorin **7**. Crude reaction mixture was dissolved in a small volume of CH_2Cl_2 and was chromatographed on 200 g of Al_2O_3 (GII). The fast moving fraction that was eluted with CH_2Cl_2 was collected (no methanol was used) and immediately was chromatographed again on 200 g of deactivated alumina (GII) using toluene as an eluent. The first blue-green fraction was collected and evaporated to give 35 mg (5.5%) of **7**. Further elution with toluene/dichloromethane mixtures allowed for separation of TPP. Finally, pure dichloromethane washed out **3** as a green fraction, which after evaporation yielded 40 mg of **3** (6.3%).

Characterization of 7. UV−vis (λ_{max} (nm), log ϵ): 424 (4.30), 525 (3.50), 563 (3.52), 630 (sh), 681 (3.80). ^{1}H NMR ($CDCl_3$, 298K) δ: 8.89 (bs, 1H, NH), 8.05 (bs, 1H, NH), 7.56 (d, 1H, ^3J = 1.1 Hz), 7.53 (2xd, 2H, ^3J = 8.2 Hz), 7.46−7.34 (m), 7.18 (m, 2H), 7.14 (m, 1H), 6.98 (m, 2H), 6.88 (d, 1H, ^3J = 5.5 Hz), 6.83 (d, 1H, ^3J = 4.8 Hz), 6.74 (d, 1H, ^3J = 5.5 Hz), 6.62 (d, 1H, ^3J = 3.9 Hz), 6.59 (d, 1H, ^3J = 3.9 Hz), 6.50 (d, 1H, ^3J = 4.8 Hz), 5.99 (s, 1H), 5.93 (d, 1H, ^3J = 1.1 Hz). ^{13}C NMR ($CDCl_3$, 298K) δ: 166.9, 147.0, 146.5, 142.9, 141.8, 140.3, 138.8, 138.2, 135.8, 134.2, 134.0, 133.4, 133.3, 132.7, 132.4, 129.4, 128.9, 128.8, 128.5, 128.4, 128.36, 128.3, 128.0, 127.9, 127.8, 127.7, 127.4, 127.3, 127.0, 124.1, 122.6, 122.4, 118.8, 117.6, 116.8, 111.9, 46.8; MS m/z_{calc}: calcd for $C_{44}H_{32}N_3S$, 634.2317; found, 634.2299.

5,10,15,20-Tetraphenyl-2-thia-21-carbaporphyrinato Chlorocadmium(II) 8. The mixture of **3** (10 mg) and anhydrous $CdCl_2$ (60 mg) was dissolved in 10 mL of $CHCl_3$ and 1 mL of freshly distilled CH_3CN. The resulting mixture was refluxed under nitrogen for 1 h. After that time, the solvents were removed with a vacuum rotary evaporator. The remaining solid was dissolved in a small

volume of dry CH_2Cl_2, and an excess of inorganic salt was removed by filtration through dense-sintered glass. Evaporation of the solvent gives cadmium complex **8** in a quantitative yield.

Characterization of 8. UV−vis (λ_{max} (nm), log ϵ): 333 (4.37), 462 (4.79), 559 (3.11), 605 (3.26), 769 (sh), 848 (4.27). ^{1}H NMR ($CDCl_3$, 298K) δ: 8.03 (AB, 1H, ^3J = 4.8 Hz), 7.98−7.95 (m, 3H), 7.92−7.89 (m, 2H), 7.75 (bs, 3H), 7.71−7.67 (m, 10H), 7.65 (m, 3H), 7.58−7.54 (m, 9H), 7.52 (AB, 1H, ^3J = 4.8 Hz), 1.72 (d, 1H, ^3J = 1.2 Hz). ^{13}C NMR ($CDCl_3$, 298K) δ: 165.7, 165.2, 160.8, 160.0, 152.8, 152.1, 146.3, 141.3, 141.1, 141.0, 140.9, 140.3, 136.19, 136.17, 135.5, 135.0, 134.8, 134.3, 134.1, 133.4, 132.6, 130.5, 129.5, 129.1, 127.5, 127.4, 127.37, 127.34, 119.0, 118.3, 88.7; HRMS m/z_{calc}: calcd for $C_{44}H_{28}N_3S^{112}Cd^+$, 744.10321; found, 744.10114.

5,10,15,20-Tetraphenyl-2-thia-21-carbaporphyrinato Chlorozinc(II) 9. Complex **3** (10 mg) was dissolved in THF (25 mL, freshly distilled from Na). To the resulting solution, an excess of $ZnCl_2$ (64 mg) and triethylamine (2 drops) were added. The mixture was stirred for 1 h. After that time, the mixture was diluted with 50 mL of dichloromethane and was washed with water (three times). The organic layer was dried with Na_2SO_4, filtered, and evaporated to give the zinc complex **9** in a quantitative yield.

Characterization of 9. UV−vis (λ_{max} (nm), log ϵ): 331 (4.39), 457 (4.88), 545 (3.03), 592 (3.19), 753 (sh), 831 (4.25). ^{1}H NMR ($CDCl_3$, 298K) δ: 8.07 (d, 1H, ^3J = 5.0 Hz), 8.01 (d, 1H, ^3J = 4.8 Hz), 7.97 (2xd, 2H, ^3J = 7.8 Hz), 7.91 (2xd, 2H, ^3J = 7.8 Hz), 7.74 (bs, 3H), 7.70−7.64 (m, 7H), 7.63−7.60 (m, 3H), 7.58−7.53 (m, 8H), 1.86 (d, 1H, ^3J = 1.1 Hz). ^{13}C NMR ($CDCl_3$, 298K) δ: 165.0, 164.7, 158.7, 158.2, 152.1, 151.7, 145.9, 141.9, 140.8, 140.6, 140.1, 135.98, 135.96, 135.2, 134.7, 134.2, 134.0, 133.2, 132.8, 132.4, 131.7, 129.4, 129.0, 127.6, 127.43, 127.39, 127.36, 127.2, 117.8, 117.3, 92.9. HRMS m/z_{calc}: calcd for $C_{44}H_{28}N_3SZn^+$, 694.12899; found 694.13015.

Instrumentation. NMR spectra were recorded on a Bruker Avance 500 spectrometer (frequencies: ^{1}H 500.13 MHz, ^{13}C 125.77 MHz, ^{113}Cd 106.05 MHz) that was equipped with either a broadband inverse gradient probehead or a direct broadband probehead. A one-dimensional (1D) variant of a gradient-selected heteronuclear single quantum correlation (HSQC) sequence was employed to record the ^{113}Cd-filtered spectra with evolution times optimized for the observed range of coupling constants. Absorption spectra were recorded on a diode array Hewlett-Packard 8453 spectrometer. Mass spectra were recorded on an AD-604 spectrometer using the electrospray and liquid matrix secondary-ion mass spectrometry techniques.

X-ray Analysis. X-ray quality crystals of **8** were prepared by diffusion of *n*-pentane into a dichloromethane solution contained in a thin tube. Data were collected at 100 K on a Kuma KM-4 charge-coupled device (CCD) diffractometer. The data were corrected for Lorentz and polarization effects. No absorption correction was applied. Crystal data are compiled in Supporting Information, Table 1. The structure was solved by direct methods with SHELXS-97 and was refined by the full-matrix least-squares method by using SHELXL-97 with anisotropic thermal parameters for the non-hydrogen atoms. Scattering factors were incorporated in SHELXS-97.[43,44] The molecule of *n*-pentane in the lattice exhibits disorder.

DFT Calculations. DFT calculations for structures **8** and **9** were performed with the GAUSSIAN 03 program.[45] Geometry optimizations were carried out within unconstrained *C*1 symmetry, with starting coordinates derived from X-ray structural data. Becke's three-parameter exchange functionals[46] with the gradient-corrected correlation formula of Lee, Yang, and Parr [DFT(B3LYP)][47] were used with the LANL2DZ basis set.[48] Harmonic vibrational frequencies were calculated using analytical second derivatives. Both structures were found to have converged to a minimum on the potential energy surface.

Topology of the electron density, ρ, was analyzed using the PROAIM package.[49]

Acknowledgment. Financial support from the Ministry of Science and Higher Education (Grant PBZ-KBN-118/T09/2004) is kindly acknowledged. M.J.C. thanks The Foundation for Polish Science for fellowship. DFT calculations were preformed at the Supercomputer Centers in Wrocław and Poznań.

Supporting Information Available: X-ray data for **8** (CIF file). Copies of 2D NMR experiments for **7** (COSY, NOESY, HMQC). Bond lengths for DFT optimized structure and Cartestian coordinates (xyz format) for **8** and **9**. Coordinates for bond critical points and ring points for **8**. This material is available free of charge via the Internet at http://pubs.acs.org.

IC061091P

(43) G. M. Sheldrick, *SHELXL97, Program for Crystal Structure Refinement*; University of Göttingen: Göttingen, Germany, 1997.
(44) G. M. Sheldrick, *SHELXS97, Program for Solution of Crystal Structures*; University of Göttingen: Göttingen, Germany, 1997.
(45) Frisch, M. J.; Trucks, G. W.; Schlegel, H. B.; Scuseria, G. E.; Robb, M. A.; Cheeseman, J. R.; Montgomery, J. A., Jr.; Vreven, T.; Kudin, K. N.; Burant, J. C.; Millam, J. M.; Iyengar, S. S.; Tomasi, J.; Barone, V.; Mennucci, B.; Cossi, M.; Scalmani, G.; Rega, N.; Petersson, G. A.; Nakatsuji, H.; Hada, M.; Ehara, M.; Toyota, K.; Fukuda, R.; Hasegawa, J.; Ishida, M.; Nakajima, T.; Honda, Y.; Kitao, O.; Nakai, H.; Klene, M.; Li, X.; Knox, J. E.; Hratchian, H. P.; Cross, J. B.; Adamo, C.; Jaramillo, J.; Gomperts, R.; Stratmann, R. E.; Yazyev, O.; Austin, A. J.; Cammi, R.; Pomelli, C.; Ochterski, J. W.; Ayala, P. Y.; Morokuma, K.; Voth, G. A.; Salvador, P.; Dannenberg, J. J.; Zakrzewski, V. G.; Dapprich, S.; Daniels, A. D.; Strain, M. C.; Farkas, O.; Malick, D. K.; Rabuck, A. D.; Raghavachari, K.; Foresman, J. B.; Ortiz, J. V.; Cui, Q.; Baboul, A. G.; Clifford, S.; Cioslowski, J.; Stefanov, B. B.; Liu, G.; Liashenko, A.; Piskorz, P.; Komaromi, I.; Martin, R. L.; Fox, D. J.; Keith, T.; Al-Laham, M. A.; Peng, C. Y.; Nanayakkara, A.; Challacombe, M.; Gill, P. M. W.; Johnson, B.; Chen, W.; Wong, M. W.; Gonzalez, C.; Pople, J. A. *Gaussian 03, Revision C.01*, Pittsburgh, PA, 2004.
(46) Becke, A. D. *Phys. Rev. A* **1988**, *38*, 3098.
(47) Lee, C.; Yang, W.; Parr, R. G. *Phys. Rev. B* **1988**, *37*, 785.
(48) Hay, P. J.; Wadt, W. R. *J. Chem. Phys.* **1985**, *82*, 270, 284, 299.
(49) Biegler-Koenig, F. W.; Bader, R. F. W.; Tang, T. H. *J. Comput. Chem.* **1982**, *3*, 317.